crystals

MDPI

Article

Fabrication of Polarization Grating on *N*-Benzylideneaniline Polymer Liquid Crystal and Control of Diffraction Beam

Mizuho Kondo [1,2,*], Kyohei Fujita [1], Tomoyuki Sasaki [2,3], Moritsugu Sakamoto [2,3], Hiroshi Ono [2,3] and Nobuhiro Kawatsuki [1,2,*]

[1] Department of Applied Chemistry, Graduate School of Engineering, University of Hyogo, 2167 Shosha, Himeji 671-2280, Japan; m1fujitak@gmail.com
[2] Japan Science and Technology Agency (JST), Core Research for Evolutional Science and Technology (CREST), Chiyoda-ku, Tokyo 102-0076, Japan; sasaki_tomoy@vos.nagaoka.ac.jp (T.S.); sakamoto@vos.nagaokaut.ac.jp (M.S.); onoh@vos.nagaokaut.ac.jp (H.O.)
[3] Department of Electrical Engineering, Nagaoka University of Technology, 1603-1 Kamitomioka, Nagaoka 940-2188, Japan
* Correspondence: mizuho-k@eng.u-hyogo.ac.jp (M.K.); kawatuki@eng.u-hyogo.ac.jp (N.K.); Tel.: +81-79-267-4014 (M.K.)

Abstract: Photoresponsive photoalignable liquid crystalline polymers composed of phenyl benzoate terminated with *N*-benzylideneaniline were evaluated. These polymers are capable of axis-selective photoreaction, photoinduced orientation, and surface relief grating formation. Polarization holography using an He-Cd laser beam at a wavelength of 325 nm demonstrated the formation of a surface relief grating with a molecularly oriented structure based on periodic light-induced reorientation and molecular motion. Electrical switching of diffracted light using an electric field response of twisted-nematic cell containing a low-molecular-weight liquid crystal in combination was also demonstrated.

Keywords: liquid crystalline polymer; axis-selective photoreaction; holography; beam diffraction

check for updates

Citation: Kondo, M.; Fujita, K.; Sasaki, T.; Sakamoto, M.; Ono, H.; Kawatsuki, N. Fabrication of Polarization Grating on *N*-Benzylideneaniline Polymer Liquid Crystal and Control of Diffraction Beam. *Crystals* **2022**, *12*, 273. https://doi.org/10.3390/cryst12020273

Academic Editors: Jun Xu, Kohki Takatoh and Akihiko Mochizuki

Received: 21 January 2022
Accepted: 15 February 2022
Published: 17 February 2022

Publisher's Note: MDPI stays neutral with regard to jurisdictional claims in published maps and institutional affiliations.

Copyright: © 2022 by the authors. Licensee MDPI, Basel, Switzerland. This article is an open access article distributed under the terms and conditions of the Creative Commons Attribution (CC BY) license (https://creativecommons.org/licenses/by/4.0/).

1. Introduction

Surface alignment patterning of optically anisotropic materials has attracted substantial attention from the perspective of science and technology because of its potential application in photonic devices for polarized light communication. In particular, polarizing gratings (PGs) have been researched and developed widely in the field of polarized beam manipulation because of their high diffraction efficiency and polarization selectivity [1,2]. These are likely to be applied to beam steering [3–6], imaging [7,8], and near-eye displays [9,10], as well as 3D displays and virtual reality/augmented reality (VR/AR) [4,11–14]. A PG is a diffractive optical element in which the in-plane anisotropic orientation varies linearly along the surface and the magnitude of anisotropy is constant [15–23]. It is fabricated by methods such as optical orientation by two-flux interference exposure [24], micro-rubbing [25,26], photomasking [27], and direct beam writing [8,28]. In these methods, the diffraction efficiency is improved by increasing the variation in refractive index in the film or the non-uniform structure of the film. Liquid crystal polymers are suitable as materials for PGs because their birefringence can be modulated substantially by external stimuli. On this, various structures have been evaluated.

In the previous study, we studied the formation of PGs by two-flux interference exposure using azobenzene [29,30] and *N*-benzylideneaniline (NBA) [31,32]. PGs are formed under interference exposure owing to the periodic distribution of light intensity and polarization state. When exposed to a polarized light beam, the azobenzene and NBA portions parallel to the polarization direction of the light beam undergo photoisomerization, followed by a trans-cis-trans reorientation process to form an oriented structure. At this time, small optical anisotropy is generated in the liquid crystal polymer film. On the other

hand, there is a significant increase in optical anisotropy when the photoirradiated film is heated above the glass transition temperature due to self-assemble mesogenic moiety with high mobility [33]. Furthermore, the NBA can be functionalized by a polymer reaction to deactivate the photoresponsive part or to increase the heat resistance by cross-linking [34]. In addition, NBA is more transparent to the visible light region than azobenzene, whereby it is more suitable for use in optical devices.

Recently, we reported an NBA polymer with a high orientation, birefringence, and high heat resistance [35]. This polymer has the capability to replace components with higher birefringence while maintaining orientation [36]. However, its application as a PG material has not been investigated. Herein, we prepared PG using this material and evaluated its diffraction properties.

2. Materials and Methods

2.1. Material

Polymethacrylate P1 coupled with phenyl benzoate terminated with NBA via a hexamethylene spacer was used (Figure 1a). P1 was synthesized by the method described in the previous literature [35]. The polymer exhibited a glass transition temperature (Tg) of 100 °C and retained its liquid crystalline phase above 295 °C. The films of the polymer were prepared by spin-coating a dichloromethane solution of the polymers onto quartz substrates.

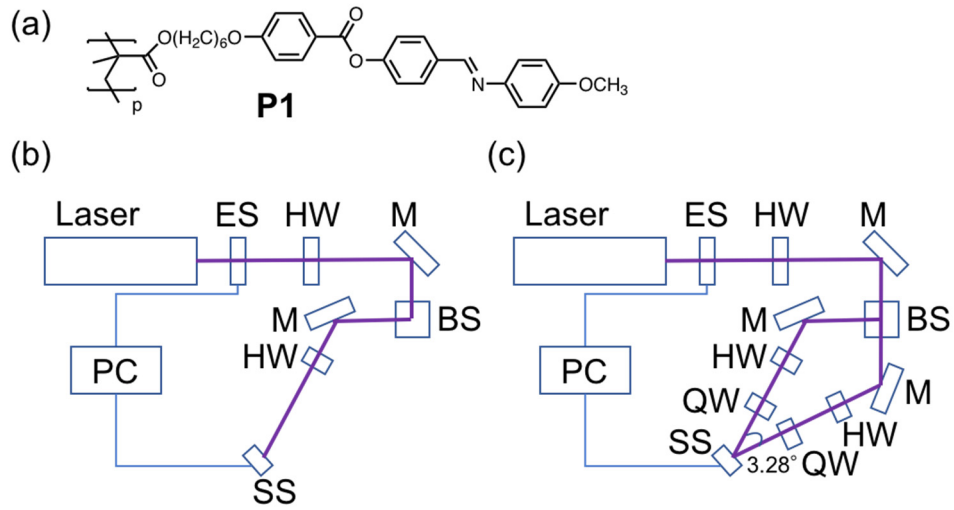

Figure 1. (**a**) Chemical structure of NBA liquid crystalline polymer P1. Experimental setup for (**b**) axis-selective photoreaction and (**c**) holographic exposure. ES, shutter; HW, half-wave plate; M, mirror; BS, beam splitter; QW, quarter wave plate; SS, sample stage; PC, personal computer.

2.2. Equipment

The photoinduced orientation behavior was evaluated by irradiating a 325 nm He-Cd laser (Kimmon IK3501R-G-S) (Tokyo, Japan) with the optical setup displayed in Figure 1b. Since the linearly polarized UV laser was emitted from the He-Cd laser source, the polarization direction of the actinic beam was controlled by a half-wave plate (HW) mounted on the rotational stage. The intensity of the laser beam was 210 mW/cm^2. The molecular orientation after linearly polarized light irradiation was evaluated using polarized absorption spectra (HITACHI U3900H) (Tokyo, Japan) and polarized light microscopy (Olympus BH-51) (Tokyo, Japan). The thermally annealed film was obtained by heating the photoirradiated film in the air at a specified temperature for 10 min.

Polarization holographic recording was performed using the experimental setup illustrated in Figure 1c. The laser beam was divided into two writing beams by a beam splitter (BS). The two writing beams with equal intensities crossed at an angle of 3.28° and impinged on the P1 films on a sample stage (SS). The resulting grating period of the polar-

ization holographic grating was estimated to be approximately 4.8 μm. The polarization states of the two writing beams were controlled individually by two quarter-wave plates. The polarization holographic gratings were written using two orthogonally circularly polarized, mutually coherent He-Cd laser beams. The intensity of the interference beam was 420 mW/cm^2. The He-Ne laser with a wavelength of 633 nm was used as a probe light to evaluate the diffraction behavior, and the diffraction efficiency was calculated using the following equation:

$$DE = I_d / I_I$$

where I_d and I_I are the intensities of the diffracted and incident beams, respectively.

The laser intensity measurement, irradiation position, and dose control were performed using a serial communication program. The surface topography was measured using an interferometer-type surface profiler (Ryoka Systems, R3300H) (Osaka, Japan). A TN cell coated with indium tin oxide (ITO) and polyimide was used for the beam switching. A liquid crystal with a low molecular weight (Merck, ZLI4792: ($\Delta n = 0.09$, $\Delta \varepsilon = 5.3$) [37]) (Darmstadt, Germany) was injected into a TN cell (EHC KSRT-04/B211PINSS05) (Tokyo, Japan) with a cell gap of 4 μm. The orientation was controlled by applying a DC voltage of 2 V using a function generator (Hokuto Denko HB-111) (Tokyo, Japan).

3. Results and Discussion

3.1. Photoalignment Behavior in Thin Films

Figure 2 shows the variation in the polarized absorption spectra of the P1 film with a thickness of 140 nm when irradiated with a single linearly polarized laser beam for 10 s as shown in Figure 1b. The absorption at 340 nm originating from the π–π* transition of NBA decreased in the direction parallel to the polarization of the laser and increased in the perpendicular direction. This indicated that the NBA moiety was rearranged perpendicular to the electric field vector of the polarized light by trans-cis-trans reorientation.

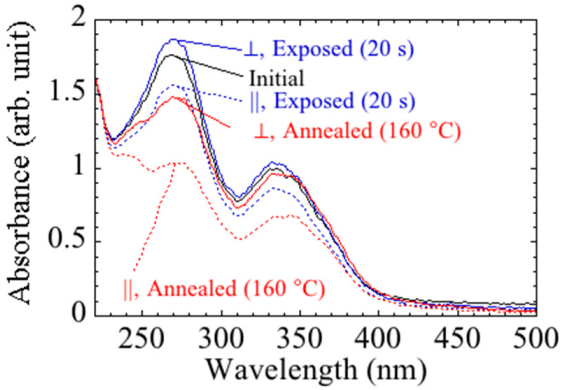

Figure 2. Polarized absorption spectra of P1 after spin-coating, irradiation with linearly polarized UV-laser, and annealing at 160 °C for 10 min. The spectra are color-coded as black for initial, blue for irradiation, and red for annealing, respectively. The absorption spectra for the directions parallel and perpendicular to the polarization direction of the laser beam are indicated by solid and dashed lines, respectively.

When heated to a temperature above the glass transition temperature, the optical anisotropy was enhanced perpendicular to the polarization direction of the laser beam. The amplified anisotropy was almost the same when the film was heated above 160 °C, while it showed a small value when the film was heated below 160 °C. The anisotropy induced by heat treatment tended to decrease for films exposed for more than 10 s. This may be due to undesired photoreactions (crosslinking or rearrangement reactions) and self-organization (out-of-plane orientation or aggregation) caused by prolonged exposure. The absorption spectra after annealing are plotted in red in Figure 2. These results are similar to those obtained under exposure to linearly polarized light from a mercury lamp [35].

Diffraction gratings were fabricated using interference exposure. Figure 3 plots the change in diffraction efficiency as a function of exposure time (solid line) and the change in diffraction efficiency of P1 films annealed at various temperatures after exposure to interference light (dashed line). The diffraction efficiency was dependent on the exposure time, increasing for exposure times shorter than 5 s and slowly decreasing for longer exposure times. The diffraction efficiency of the P1 film was stable after switching off the interfering beams though the diffraction efficiency after irradiation was very low (<0.5%). On the other hand, it was remarkably improved by heating above the glass transition temperature. The diffraction efficiency increased to 3.8% for the film exposed for 5 s at 240 °C. These can be attributed to the amplification of orientation and the expansion of birefringence modulation by heating and polarized laser irradiation. However, the diffraction efficiency was marginal (<5%), possibly due to the small film thickness.

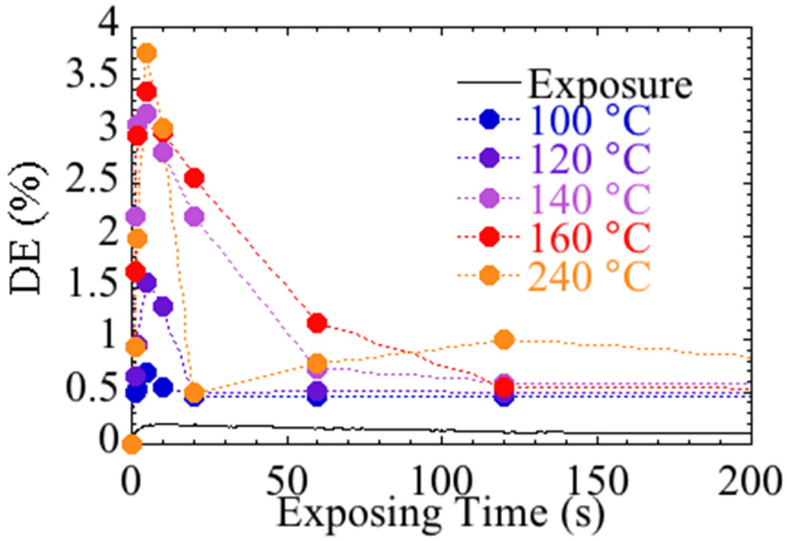

Figure 3. Variation in +1st diffraction efficiency of P1 film as a function of exposure time (solid line) and 1st diffraction efficiency of P1 film after thermal annealing under various temperatures (dashed lines).

The surface morphology of the heat-treated films was also evaluated. Periodic irregularities with a pitch of approximately 4 μm and a height difference of approximately 40 nm were observed after heat treatment. This indicated that the height difference was caused by the diffraction grating formation (Figure 4a). The surface relief was formed by the mass transfer of NBA upon light irradiation. This mechanism is identical to that of azobenzene and indicates that the diffractive structure is formed by a behavior identical to that of conventional NBA polymers. Figure 4b shows a polarized light micrograph of the diffraction grating. Periodic bright stripes are observed along the diffraction grating vector. This indicates that the NBA is arranged periodically and that the refractive index varies periodically. To investigate the optical anisotropy caused by the molecular arrangement, the grating was observed by rotating the polarizer and analyzer simultaneously by 30° while maintaining the grating fixed. The results showed that the rotation of the polarizer and analyzer caused the bright stripes to shift along the grating vector and recovered to the initial pattern at 180°. This indicates that the polarization direction of the linearly polarized light is modulated periodically by the interference of two orthogonal circularly polarized beams (Figure 4c) [38].

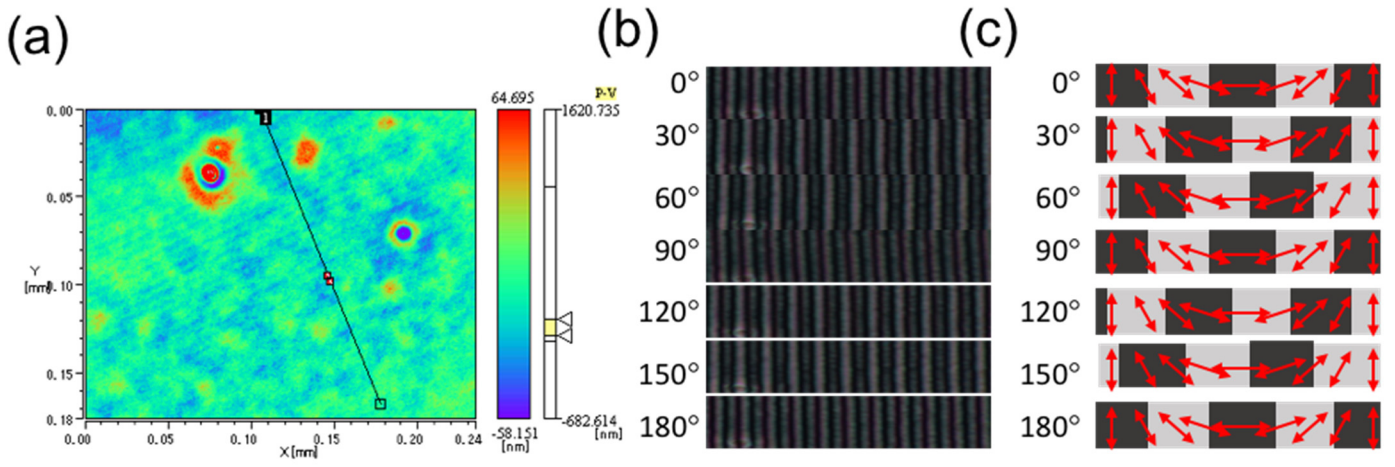

Figure 4. (**a**) Surface profile of P1 after irradiation with interference beams following thermal annealing (5 s, 240 °C). (**b**) Polarizing micrographs observed as a function of the rotation angle of the polarizer and analyzer, θ. (**c**) Alignment of mesogens induced in holograms. The arrows indicate the direction of mesogens. The white and gray areas correspond to the bright and dark areas, respectively, in (**c**).

3.2. Photoalignment Behavior in Thick Films

Figure 5a shows the polarization absorption spectra of a 460 nm-thick film after irradiation with LP-325 nm and heat treatment. Similar to the 140 nm film, the absorption in the direction parallel to the polarization field decreased with UV irradiation. However, a marginal amplification was induced by thermal annealing. Figure 5b shows the diffraction efficiencies of the films after interference exposure for various times. The diffraction efficiency after irradiation with the interference beam increased compared with that of the thin film. However, the increase after thermal treatment was marginal. Figure 5c shows the polarized light micrographs of the diffraction gratings. These show periodic bright stripes along the grating vectors as in the 140 nm film. However, the periodic structure is disrupted marginally after thermal treatment. The surface morphology of the film shows that the surface layer of the film became rougher after heat treatment. When this experiment was conducted using a significantly thicker film (900 nm), diffraction structures disappeared after heat treatment (data not shown). These results indicate that the thicker film increases the number of areas in the deeper layers of the film that are not involved in optical orientation. This, in turn, induces unintended self-organization and orientation (e.g., out-of-plane orientation), thereby resulting in surface roughening and a decrease in anisotropy. Meanwhile, reorientation is partially induced in the surface layer of the film by heat treatment. This is expected to increase the diffraction efficiency. It is necessary to reexamine the composition of the film (e.g., the transmittance and the introduction of a structure that facilitates reorientation) to increase the diffraction efficiency.

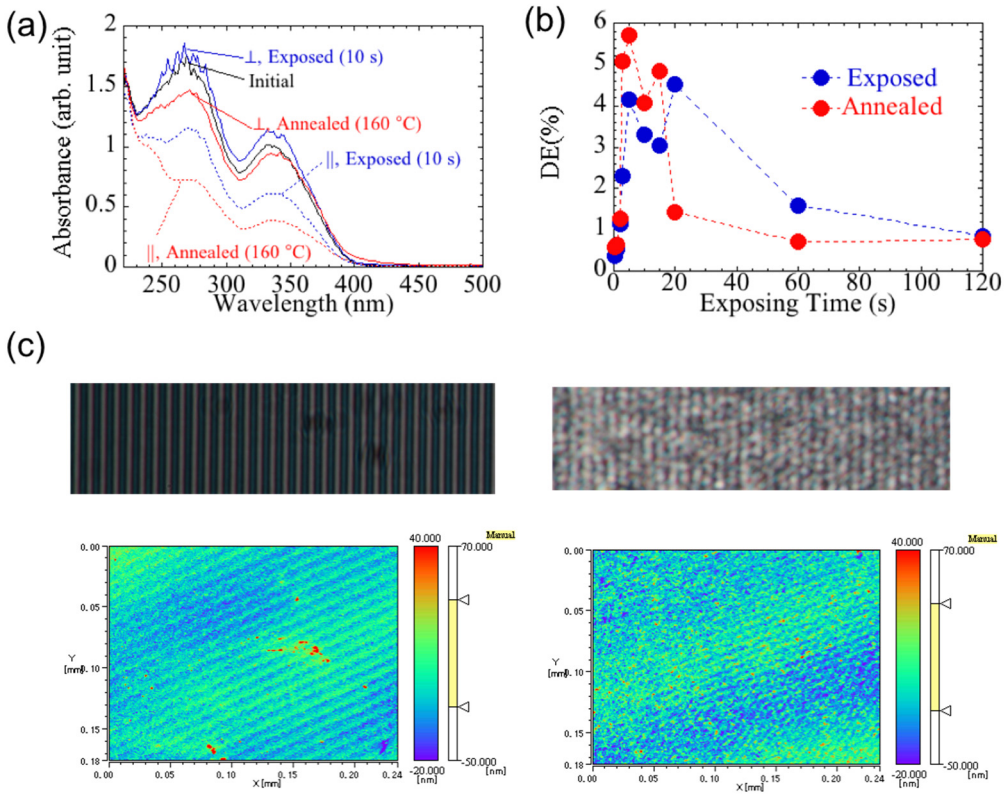

Figure 5. (**a**) Polarized absorption spectra of P1 film with a thickness of 460 nm after spin-coating, irradiation with linearly polarized UV-laser, and annealing at 160 °C for 10 min. The spectra are color-coded as black for initial, blue for irradiation, and red for annealing, respectively. The absorption spectra for the directions parallel and perpendicular to the polarization direction of the laser beam are indicated as solid and dashed lines, respectively. (**b**) Variation in +1st diffraction efficiency of P1 film with a thickness of 460 nm as a function of exposure time (solid line) and 1st diffraction efficiency of P1 film after thermal annealing at 160 °C. (**c**) POM image (**top**) and surface profile (**bottom**) of P1 film with thickness of 460 nm after irradiation (**left**) and thermal annealing (**right**).

3.3. Diffraction Control Using TN Cell

The combination of a field-driven cell and quarter-wave plate enables switching of the laser [39,40]. In particular, an optical system combining a field-driven TN cell and quarter-wave plate can switch the diffracted light from the +1st order to the −1st order, or vice versa, by controlling the voltage applied to the TN cell [4]. In this method, multiple diffraction angles can be obtained by cascading multiple PGs, and simultaneous wavelength control is feasible. Two-dimensional directional control is also likely to be feasible owing to the transmission type and cascade connection capability. Figure 6a,b shows the diffraction images of the voltage-off and voltage-on states, respectively (support Video S1). For the polarization grating, we used a 140 nm P1 film after thermal annealing. As expected, the diffraction order varies from +1 to −1 and vice versa. Since it is intended to be controlled by a single-board computer, DC voltage control is used; however, simple AC voltage (4 V, 60 Hz) can also be used for control (support Figure S1). Efficient switching is likely to be achieved by improving the diffraction efficiency. This is presently under study.

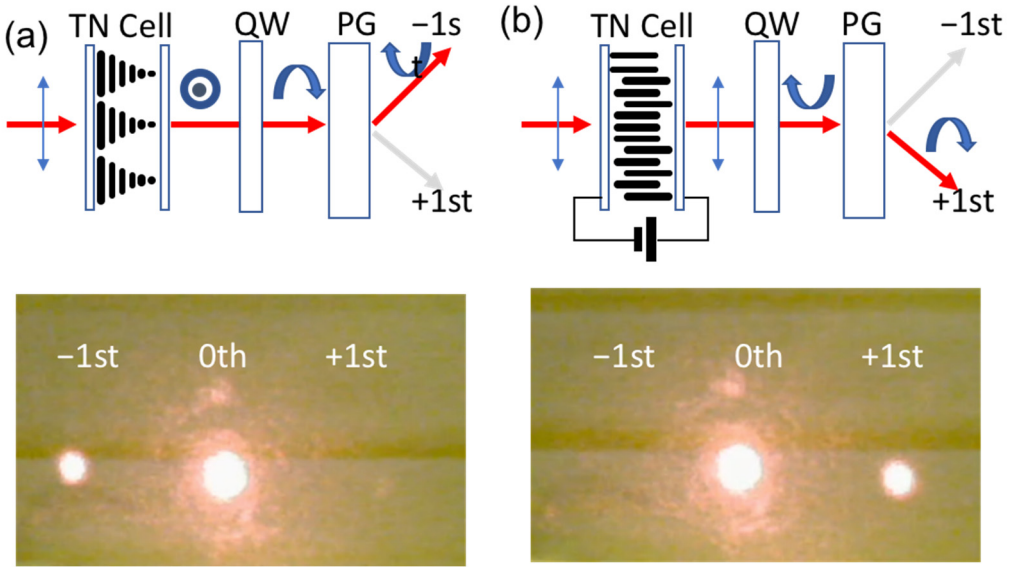

Figure 6. Schematic diagram (**top**) and photograph of diffraction (**bottom**) of proposed optical switch based on PG at (**a**) voltage-off state and (**b**) voltage-on state.

4. Conclusions

Axis-selective photoreaction, photoinduced orientation, and surface relief grating formation were evaluated using liquid crystalline polymers composed of phenyl benzoate terminated with NBA. Heat treatment greatly amplifies the molecular arrangement in the photo-reactive thin film, while the amplification is small in the photo-reactive thick film. The formation of a polarization grating with a molecularly oriented structure based on periodic light-induced reorientation and molecular motion was demonstrated. We demonstrated the electrical switching of diffracted light using a TN cell. Although the transmission of zero-order light could not be prevented in this study, more efficient beam control is likely to be achieved by biasing the diffraction of first-order light through the formation of a more efficient diffraction grating. It is necessary to reexamine the composition of the film, such as the transmittance and the introduction of a structure that facilitates reorientation.

Supplementary Materials: The following are available online at https://www.mdpi.com/article/10.3390/cryst12020273/s1, Figure S1: Diffraction photographs of an optical switch using an AC input (4 V, 60 Hz), Video S1: Switching of diffracted beam using field-driven cell.

Author Contributions: Conceptualization, N.K. and M.K.; Methodology, M.K.; Software, M.K.; Validation, K.F., M.K.; Investigation, K.F.; Optical setup, H.O., T.S., M.S.; Resources, N.K.; Writing—original draft preparation, M.K.; Writing—review and editing, N.K.; Visualization, M.K.; Supervision, N.K. All authors have read and agreed to the published version of the manuscript.

Funding: This research received no external funding.

Acknowledgments: This work was supported by Japan Science and Technology Agency (CREST JPMJCR2101).

Conflicts of Interest: The authors declare no conflict of interest.

References

1. Lin, T.; Xie, J.; Zhou, Y.; Zhou, Y.; Yuan, Y.; Fan, F.; Wen, S. Recent Advances in Photoalignment Liquid Crystal Polarization Gratings and Their Applications. *Crystals* **2021**, *11*, 900. [CrossRef]
2. Nersisyan, S.R.; Tabiryan, N.V.; Steeves, D.M.; Kimball, B. Optical Axis Gratings in Liquid Crystals and their use for Polarization insensitive optical switching. *J. Nonlinear Opt. Phys. Mater.* **2009**, *18*, 1–47. [CrossRef]
3. Oh, C.; Kim, J.; Muth, J.; Serati, S.; Escuti, M.J. High-Throughput Continuous Beam Steering Using Rotating Polarization Gratings. *IEEE Photonics Technol. Lett.* **2010**, *22*, 200–202. [CrossRef]

4. Chen, H.; Weng, Y.; Xu, D.; Tabiryan, N.V.; Wu, S.-T. Beam steering for virtual/augmented reality displays with a cycloidal diffractive waveplate. *Opt. Express* **2016**, *24*, 7287–7298. [CrossRef]
5. Tabirian, N.V.; Roberts, D.; Liao, Z.; Ouskova, E.; Sigley, J.; Tabirian, A.; Slagle, J.; McConney, M.; Bunning, T.J. Size, weight, and power breakthrough in nonmechanical beam and line-of-sight steering with geo-phase optics. *Appl. Opt.* **2021**, *60*, G154–G161. [CrossRef]
6. Kim, J.; Oh, C.; Serati, S.; Escuti, M.J. Wide-angle, nonmechanical beam steering with high throughput utilizing polarization gratings. *Appl. Opt.* **2011**, *50*, 2636–2639. [CrossRef]
7. Kudenov, M.W.; Escuti, M.J.; Dereniak, E.L.; Oka, K. White-light channeled imaging polarimeter using broadband polarization gratings. *Appl. Opt.* **2011**, *50*, 2283–2293. [CrossRef]
8. Ono, H.; Wada, T.; Kawatsuki, N. Polarization imaging screen using vector gratings fabricated by photocrosslinkable polymer liquid crystals. *Jpn. J. Appl. Phys.* **2012**, *51*, 030202. [CrossRef]
9. Xiong, J.; Tan, G.; Zhan, T.; Wu, S.-T. Wide-view augmented reality display with diffractive cholesteric liquid crystal lens array. *J. Soc. Inf. Disp.* **2020**, *28*, 450–456. [CrossRef]
10. Zhan, T.; Zou, J.; Xiong, J.; Liu, X.; Chen, H.; Yang, J.; Liu, S.; Dong, Y.; Wu, S.-T. Practical Chromatic Aberration Correction in Virtual Reality Displays Enabled by Cost-Effective Ultra-Broadband Liquid Crystal Polymer Lenses. *Adv. Opt. Mater.* **2020**, *8*, 1901360. [CrossRef]
11. Zhan, T.; Lee, Y.-H.; Wu, S.-T. High-resolution additive light field near-eye display by switchable Pancharatnam–Berry phase lenses. *Opt. Express* **2018**, *26*, 4863–4872. [CrossRef]
12. Zhan, T.; Xiong, J.; Tan, G.; Lee, Y.-H.; Yang, J.; Liu, S.; Wu, S.-T. Improving near-eye display resolution by polarization multiplexing. *Opt. Express* **2019**, *27*, 15327–15334. [CrossRef]
13. Xiong, J.; Wu, S. Rigorous coupled-wave analysis of liquid crystal polarization gratings. *Opt. Express* **2020**, *28*, 35960–35971. [CrossRef]
14. Wang, Q.-H.; Ji, C.-C.; Li, L.; Deng, H. Dual-view integral imaging 3D display by using orthogonal polarizer array and polarization switcher. *Opt. Express* **2016**, *24*, 9–16. [CrossRef]
15. Lee, Y.-H.; Yin, K.; Wu, S.-T. Reflective polarization volume gratings for high efficiency waveguide-coupling augmented reality displays. *Opt. Express* **2017**, *25*, 27008–27014. [CrossRef]
16. Packham, C.; Escuti, M.; Ginn, J.; Oh, C.; Quijano, I.; Boreman, G. Polarization Gratings: A Novel Polarimetric Component for Astronomical Instruments. *Public. Astron. Soc. Pac.* **2011**, *122*, 1471–1478. [CrossRef]
17. Nikolova, L.; Todorov, T. Diffraction efficiency and selectivity of polarization holographic recording. *Opt. Acta* **1984**, *31*, 579–588. [CrossRef]
18. Bomzon, Z.; Biener, G.; Kleiner, V.; Hasman, E. Space-variant Pancharatnam-Berry phase optical elements with computer-generated subwavelength gratings. *Opt. Lett.* **2002**, *27*, 1141–1143. [CrossRef]
19. Gori, F. Measuring Stokes parameters by means of a polarization grating. *Opt. Lett.* **1999**, *24*, 584–586. [CrossRef]
20. Roberts, D.; Kaim, S.; Tabiryan, N.V.; McConney, M.; Bunning, T.J. Polarization-independent diffractive waveplate optics. In Proceedings of the 2018 IEEE Aerospace Conference, Big Sky, MT, USA, 3–10 March 2018; pp. 1–11.
21. Tabiryan, N.; Roberts, D.; Steeves, D.; Kimball, B. 4G Optics: New Technology Extends Limits to the Extremes. *Photonics Spectra* **2017**, *51*, 46–50.
22. Tabiryan, N.V.; Roberts, D.E.; Liao, Z.; Hwang, J.; Moran, M.; Ouskova, O.; Pshenichnyi, A.; Sigley, J.; Tabirian, A.; Vergara, R.; et al. Advances in Transparent Planar Optics: Enabling Large Aperture, Ultrathin Lenses. *Adv. Opt. Mater.* **2021**, *9*, 2001692. [CrossRef]
23. Nersisyan, S.R.; Tabiryan, N.V.; Steeves, D.M.; Kimball, B.R. The Promise of Diffractive Waveplates. *Opt. Photonics News* **2010**, *21*, 41–45. [CrossRef]
24. Zhan, T.; Lee, Y.-H.; Tan, G.; Xiong, J.; Yin, K.; Gou, F.; Zou, J.; Zhang, N.; Zhao, D.; Yang, J.; et al. Pancharatnam-Berry optical elements for head-up and near-eye displays. *J. Opt. Soc. Am. B* **2019**, *36*, D52–D65. [CrossRef]
25. Honma, M.; Nose, T. Twisted nematic liquid crystal polarization grating with the handedness conservation of a circularly polarized state. *Opt. Express* **2012**, *20*, 18449–18458. [CrossRef] [PubMed]
26. Honma, M.; Nose, T. Highly efficient twisted nematic liquid crystal polarization gratings achieved by microrubbing. *Appl. Phys. Lett.* **2012**, *101*, 041107. [CrossRef]
27. Hisano, K.; Ota, M.; Aizawa, M.; Akamatsu, N.; Barrett, C.J. Shishido, A. Single-step creation of polarization gratings by scanning wave photopolymerization with unpolarized light. *J. Opt. Soc. Am. B* **2019**, *36*, D112–D118. [CrossRef]
28. Noda, K.; Kawai, K.; Sasaki, T.; Kawatsuki, N.; Ono, H. Multilevel anisotropic diffractive optical elements fabricated by means of stepping photo-alignment technique using photo-cross-linkable polymer liquid crystals. *Appl. Opt.* **2014**, *53*, 2556. [CrossRef]
29. Emoto, A.; Wada, T.; Shioda, T.; Sasaki, T.; Manabe, S.; Kawatsuki, N.; Ono, H. Vector gratings fabricated by polarized rotation exposure to hydrogen-bonded liquid crystalline polymers. *Jpn. J. Appl. Phys.* **2011**, *50*, 032502. [CrossRef]
30. Sasaki, T.; Izawa, M.; Noda, K.; Nishioka, E.; Kawatsuki, N.; Ono, H. Temporal formation of optical anisotropy and surface relief during polarization holographic recording in polymethylmethacrylate with azobenzene side groups. *Appl. Phys. B Lasers Opt.* **2014**, *114*, 373–380. [CrossRef]

31. Sasaki, T.; Nishioka, E.; Noda, K.; Kondo, M.; Kawatsuki, N.; Ono, H. Analysis of Non-Sinusoidal Surface Relief Structures Induced by Elliptical Polarization Holography on Azobenzene-Containing Polymeric Films. *Jpn. J. Appl. Phys.* **2014**, *53*, 02BB06. [CrossRef]
32. Kawatsuki, N.; Hosoda, R.; Kondo, M.; Sasaki, T.; Ono, H. Molecularly oriented surface relief formation in polymethacrylates comprising N-benzylideneaniline derivative side groups. *Jpn. J. Appl. Phys.* **2014**, *53*, 128002. [CrossRef]
33. Kawatsuki, N. Photoalignment and Photoinduced Molecular Reorientation of Photosensitive Materials. *Chem. Lett.* **2011**, *40*, 548–554. [CrossRef]
34. Ito, A.; Norisada, Y.; Inada, S.; Kondo, M.; Sasaki, T.; Sakamoto, M.; Ono, H.; Kawatsuki, N. Photoinduced Reorientation and Photofunctional Control of Liquid Crystalline Copolymers with in Situ-Formed N-Benzylideneaniline Derivative Side Groups. *Langmuir* **2021**, *37*, 1164–1172. [CrossRef] [PubMed]
35. Nisizono, T.; Kondo, M.; Kawatsuki, N. Photoinduced Molecular Reorientation of a Liquid Crystalline Polymer with a High Birefringence. *Chem. Lett.* **2021**, *50*, 912–915. [CrossRef]
36. Sakai, A.; Nnishizono, T.; Kondo, M.; Sasaki, T.; Sakamoto, M.; Ono, H.; Kawatsuki, N. Birefringence control of photoalignable liquid crystalline polymers based on an in situ exchange of oriented mesogenic side groups. *Chem. Lett.* **2021**, *50*, 91–93. [CrossRef]
37. Yamaguchi, R.; Sasaki, R.; Inoue, K. Driving Voltage in Reverse Mode Cell Using Reactive Mesogen: Effect of UV Absorption of Liquid Crystal. *J. Photopolm. Sci.* **2018**, *31*, 301. [CrossRef]
38. Shishido, A.; Ishiguro, M.; Ikeda, T. Circular Arrangement of Mesogens Induced in Bragg-type Polarization Holograms of Thick Azobenzene Copolymer Films with a Tolane Moiety. *Chem. Lett.* **2007**, *36*, 1146–1147. [CrossRef]
39. Sarkissian, H.; Serak, S.V.; Tabiryan, N.V.; Glebov, L.B.; Rotar, V.; Zeldovich, B.Y. Polarization- controlled switching between diffraction orders in transverse-periodically aligned nematic liquid crystals. *Opt. Lett.* **2006**, *31*, 2248–2250. [CrossRef]
40. Wu, S.T.; Efron, U.; Hess, L.D. Birefringence measurements of liquid crystals. *Appl. Opt.* **1984**, *23*, 3911–3915. [CrossRef]